Electrical Engineering in Japan, Vol. 117, No. 6, 1996
Translated from Denki Gakkai Ronbunshi, Vol. 115-B, No. 11, November 1995, pp. 1297-1303

Improvement of Power System Stability Using Multivariable Excitation Control

KAIICHIRO HIRAYAMA and YUICHI UEMURA
Toshiba Corporation

SUMMARY

Improvement of power system stability is the most important issue of generator excitation control. The combination of thyristor excitation with ΔP-PSS is usually applied to recently installed very large turbogenerators. This power system generator (PSS) is not always effective for wide-range operation of generators or for various changes of power system line impedance. The application of the optimal control theory, especially the multifeedback signal resulting from the Riccati equation has been studied and reported in many papers. These papers, however, do not clearly describe how to set performance index values and the studies reported in them also use inadequate signals. This paper presents a method to set the performance index values to make adequate feedback signals for selecting actual control on the application of the Riccati equation. Further, the developed PSS using multifeedback signals is applied to actual very large turbogenerators after confirming the performance of effective damping for power oscillation.

Key words: Power system stability; lower excitation control; power system stabilizer (PSS); automatic voltage regulator (AVR); multivariable control; Riccati equation.

1. Introduction

With electric power networks growing in size, certain efforts have been made to improve generator stability. In most large-size generators in operation, power system stabilizers with active power, serving as input (Δ-PSS), are usefully employed. Those power system stabilizers are based on gain and lead/lag compensation functions, and analytical methods have been worked out to set coefficients for gain and lead/lag [1]. The PSS have been studied using optimal control to offer wider dynamic stability areas, and better damping of power oscillation as compared to ΔP-PSS, such as reported in [2, 3, 4, 5]. These papers offer considerations and results concerning optimal control methods using state feedback obtained by solving Riccati equations. The methods reported allow the evaluation function to be optimized, provided all state variables can be included through associated signals. There are papers [6, 7, 8, 9] reporting on some methods that are applicable to actual control units, but these methods are hardly practicable as PSS since they use phase shift angle for one of the feedback signals. The reports also leave unexplained how the evaluation function of the Riccati equation should be set to reach the desirable PSS effect.

In the context of applicability to actual machines, PSS control constants are so set that damping torque approximates a certain target value [1]. If in doing so, phase shift angle feedback signal can be made negligibly small, and damping torque can be employed as with conventional PSS design, it is possible to calculate appropriate feedback parameters based on conditions of generators and other system elements in order to obtain desired damping torque.

A method is proposed to design multivariable control PSS, applicable to actual generator excitation control units, using multiple feedback signals obtained through setting an evaluation function that supports, first, selecting reliable signals and, second, producing specified damping torque, and then solving the Riccati equation.

To make sure that multivariable control PSS designed with this method ensures stability improvement

ISSN0424-7760/97/0006-0043

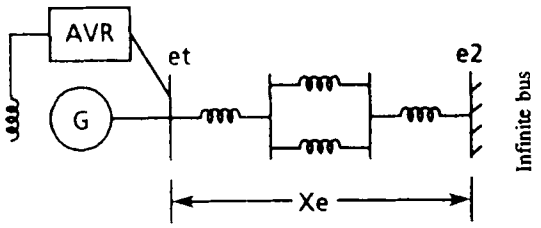

Fig. 1. One-machine-to-infinite-bus power system.

as desired, damping torque and dynamic stability were calculated across an appropriate bandwidth, and the results have confirmed sufficient robustness. Positive results were also obtained in estimation of power oscillation damping effect of multivariable control PSS in a one-machine-to-infinite-bus system, using transient response calculations.

To obtain a comparative estimation, transient stability was calculated for three-generator configurations using multivariable control PSS and ΔP-PSS, the field test was conducted by application of multivariable control PSS to a large-size generator, with good results achieved.

2. Application of Control Theory

2.1 Model of generator and excitation system

Using a multigenerator system model is desirable to set control constants for multivariable control PSS. In real power systems, however, adjacent generators may often happen to employ different excitation schemes such as thyristor excitation, ac excitation, etc.; this results in different excitation control response speed and PSS characteristics. Because of this, consideration of one-machine-to-infinite-bus configuration seems more realistic. Hence, multivariable control PSS was designed for generator excitation control with the system configuration as shown in Fig. 1.

Represented in Fig. 2 is linear approximation of the one-machine-to-infinite-bus system under a microvariation about the operating point [1].

In Fig. 2, $K_1 \sim K_6$ are coefficients determined by generator's characteristics, operating conditions, system impedance Xe and infinite bus voltage e_2. Designated as $G(S)$ is the AVR transfer function to control generator's voltage. The transmission line impedance Xe is 0.4 p.u. including the impedance of generator's transformer. At normal operating point of the generator under rated active power, reactive power is 0.1 p.u. and this operating point was taken for multivariable control PSS calculations. Using constants listed in Table 1, and assuming the terminal voltage to be 1 p.u., the following values for $K_1 \sim K_6$ were calculated:

$K_1 = 1.22$P.U, $K_2 = 1.42$P.U, $K_3 = 0.32$P.U
$K_4 = 0.65$P.U, $K_5 = -0.28$P.U, $K_6 = 0.55$P.U

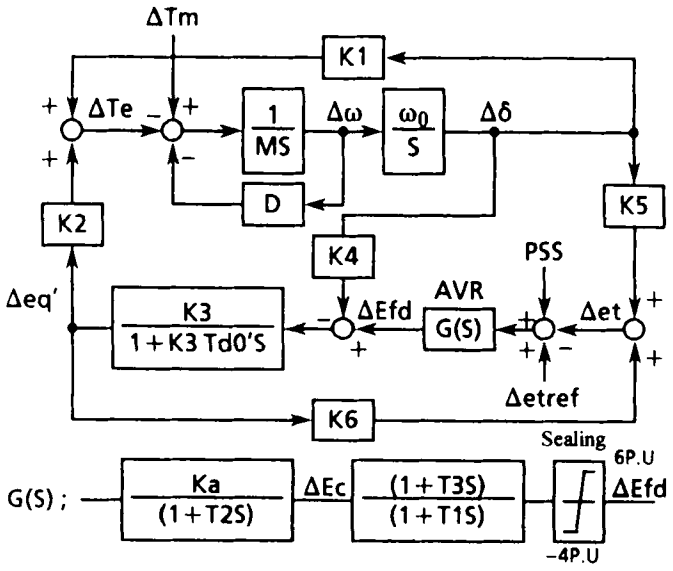

Fig. 2. Block diagram of system under study.

2.2 Development of mathematical model

In case of excitation control in the block diagram of Fig. 2, with operation of mechanical system being ignored, and assuming $\Delta T_m = 0$, Eqs. (1)-(7) can be derived:

$$\Delta\omega = \frac{-(\Delta T_e + D\Delta\omega)}{MS} \tag{1}$$

$$\Delta\delta = \frac{\omega_0 \Delta\omega}{S} \tag{2}$$

$$\Delta e'_q = \frac{K_3 \Delta E_{fd}}{(1+K_3 T_{do'} S)} - \frac{K_3 K_4 \Delta\delta}{(1+K_3 T_{do'} S)} \tag{3}$$

$$\Delta T_e = K_1 \Delta\delta + K_2 \Delta e'_q \tag{4}$$

$$\Delta e_t = K_5 \Delta\delta + K_6 \Delta e'_q \tag{5}$$

$$\Delta E_{fd} = \frac{(1+T_3 S)}{(1+T_1 S)} \Delta E_c \tag{6}$$

$$\Delta E_c = \frac{K_a (\Delta et_{ref} - \Delta e_t)}{(1+T_2 S)} \tag{7}$$

The symbol Δ suggests a variable's increment, and S is Laplacian.

With $\Delta e'_q$, Δe_t excluded from Eqs. (1)-(7), the following state equation is obtained:

$$\dot{\mathbf{x}} = \mathbf{A}\mathbf{x} + \mathbf{b} \cdot \mathbf{u} \tag{8}$$

Here, x, A, B, u are defined as follows.

$$\mathbf{x}^t = (\Delta\omega,\ \Delta\delta,\ \Delta E_c,\ \Delta E_{fd},\ \Delta T_e) \tag{9}$$

$$\mathbf{A} = \begin{pmatrix} -\frac{D}{M} & 0 & 0 & 0 & -\frac{1}{M} \\ \omega_0 & 0 & 0 & 0 & 0 \\ 0 & a_1 & a_4 & 0 & a_8 \\ 0 & a_2 & a_5 & a_6 & a_9 \\ K_1\omega_0 & a_3 & 0 & a_7 & a_{10} \end{pmatrix}$$

$$a_1 = \frac{K_a\left(\frac{K_1 K_6}{K_2} - K_5\right)}{T_2}$$

Table 1. Constants of generator and AVR

Generator's constants
Xd=1.7P.U Xd'=0.28P.U
Xq=1.7P.U Tdo'=5.6 s
M (inertia constant) = 7 s
D (intrinsic damping torque) = 3P.U
f=50HZ (ω_0=314rad / s)
(800MVA base value)
AVR's constants
T_1=0.032 s, T_2=1.11 s
T_3=0.33 s, K_a=200

$$a_2 = \frac{K_a T_3\left(\frac{K_1 K_6}{K_3} - K_5\right)}{T_1 T_2}, \quad a_3 = \frac{\frac{K_1}{K_3} - K_2 K_4}{T_{do'}}$$

$$a_4 = -\frac{1}{T_2}, \quad a_5 = \frac{T_2 - T_3}{T_1 T_2}$$

$$a_6 = -\frac{1}{T_1}, \quad a_7 = \frac{K_2}{T_{do'}}$$

$$a_8 = \frac{-K_a K_6}{T_2 K_2}, \quad a_9 = -\frac{K_a T_3 K_6}{T_1 T_2 K_2}$$

$$a_{10} = -\frac{1}{T_{do'} K_3}$$

$\mathbf{b}^t = (0,\ 0,\ b3,\ b4,\ 0)$

$$b_3 = \frac{K_a}{T_2}, \quad b_4 = \frac{K_a T_3}{T_1 T_2}$$

$\mathbf{u} = \Delta etref$

Given here is the Riccati equation [3]:

$$\mathbf{A}^t\mathbf{P} + \mathbf{P}\mathbf{A} - \mathbf{P}\mathbf{b}\mathbf{R}^{-1}\mathbf{b}^t\mathbf{P} + \mathbf{Q} = 0 \tag{11}$$

The evaluation function J is represented by

$$J = 0.5 \int_0^\infty (\mathbf{x}^t\mathbf{Q}\mathbf{x} + \mathbf{u}^t\mathbf{R}\mathbf{u})\, dt \tag{12}$$

The weight function Q for x in the state equation (8) may

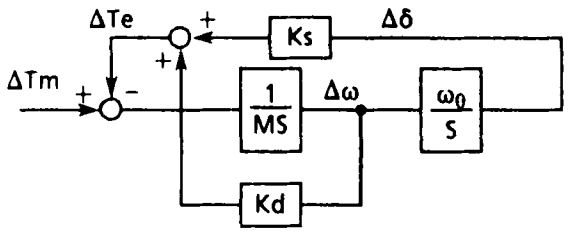

Fig. 3. Generalized block diagram for dynamic stability.

be represented with diagonal matrix as follows:

$$\mathbf{Q}=\mathrm{diag}\,(q_w,\ q_e,\ q_c,\ q_f,\ q_p) \tag{13}$$

Hence, the feedback signal may be written as follows:

$$\mathbf{u}=-\mathbf{R}^{-1}\mathbf{b}^t\mathbf{P}\mathbf{x} \tag{14}$$

This feedback gain **u** is found through specifying **Q**, and solving Eqs. (11)-(14).

3. Specification of Evaluation Function with Regard to Stability

3.1 Specification of attenuation coefficient ζ

Shown in Fig. 3 is a generalization of the block diagram (Fig. 2) with only ΔT_m, ΔT_e, $\Delta\omega$, $\Delta\delta$ left [1].

Vibration equation for Fig. 3 may be represented as follows:

$$S^2+2\zeta\omega'_n\,S+\omega'^2_n=0 \tag{15}$$

while the characteristic equation is as follows:

$$S^2+\frac{K_d}{M}S+\frac{\omega_0 K_S}{M}=0 \tag{16}$$

Coefficients K_d and K_s are referred to as damping torque coefficient and synchronizing torque coefficient, respectively. These coefficients allow for influences from AVR, including PSS. With Eq. (16) compared to Eq. (15), and ζ *and* ω'_n represented through the coefficients of Eq. (16), the following Eqs. (17), (18) can be derived:

$$\zeta=\frac{K_d}{2M\omega'_n} \tag{17}$$

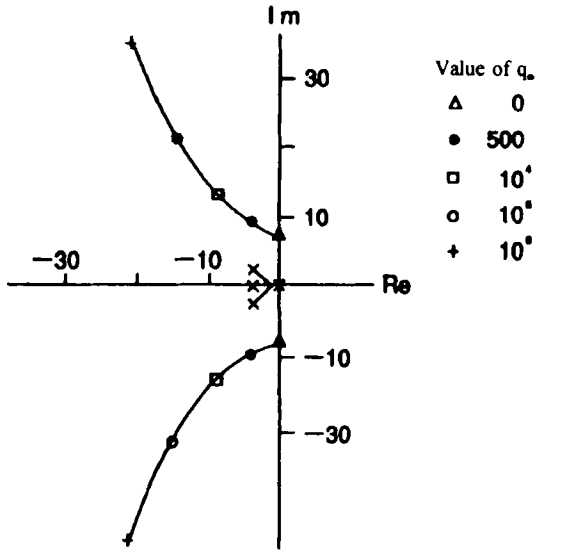

Fig. 4. Root locus with q_∞ taken as parameter.

$$\omega'_n=\sqrt{\frac{\omega_0 K_S}{M}} \tag{18}$$

With d-axis flux linkage in Fig. 2 being constant, natural frequency ω_n may be represented as follows [10], by analogy with Eq. (15):

$$\omega_n=\sqrt{\frac{\omega_0 K_1}{M}} \tag{19}$$

Since this ω_n approximates ω'_n of Eq. (18) [1], ω'_n gets determined as soon as K_1 is calculated. Just as with conventional ΔP-PSS, the coefficient K_d in Eq. (16) is set to $K_d \geq 30$. By rearranging Eq. (17), the following can be obtained:

$$K_d=2\zeta M\omega'_n \fallingdotseq 2\zeta M\omega_n \geqq 30 \tag{20}$$

Now substitute $K_1 = 1.22$ as well as the values of Table 1 for M, ω_0, into Eq. (19):

$$\omega_n=7.4\,\mathrm{rad/s}$$

As a result $\zeta \geq 0.29$ and, therefore, ζ is set to 0.3 or more.

Table 2. Calculation of ζ with q_ω as parameter

q_ω	$\alpha \pm j\beta$	ζ
100	-1.5±8.2	0.18
500	-3.2±j8.7	0.35
10^4	-8.7±j12.9	0.56
10^5	-14.3±j21.2	0.56
10^6	-20.1±j33.4	0.52

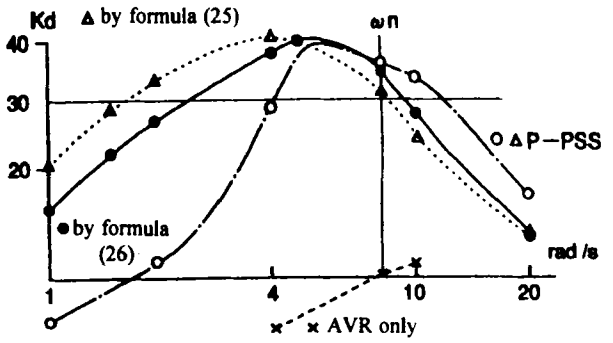

Fig. 5. Frequency characteristic of damping torque coefficient.

3.2 Specification of evaluation function

As shown in Fig. 3, the damping torque coefficient K_d varies directly with rotational speed. Therefore, taking q_e, q_c, q_r, q_p for zero in Eq. (11), and giving weight only to $\Delta\omega$ in Eq. (12), the evaluation function is represented as follows.

$$J = 0.5 \int_0^\infty (q_\omega \Delta\omega^2 + u^2)\, dt \qquad (21)$$

The key point here is how to set q_ω. Figure 4 presents root locus calculated with q_ω taken as parameter.

Denoting the root locus as complex number of $-\alpha \pm j\beta$, the following quadratic equation can be written for S:

$$S^2 + 2\alpha S + \alpha^2 + \beta^2 = 0 \qquad (22)$$

Proceeding from Eqs. (15) and (22):

$$\zeta = \frac{\alpha}{\omega'_n}, \quad \omega'_n = \sqrt{\alpha^2 + \beta^2} \qquad (23)$$

Presented in Table 2 are results of calculation of ζ using Eq. (23) for various values of q_ω.

From Table 2, $q_\omega = 500$ is selected as the best value to meet the aforementioned condition of $\zeta \geq 0.3$. Therefore, Eq. (21) for evaluation function takes the following appearance:

$$J = 0.5 \int_0^\infty (500\Delta\omega^2 + u^2)\, dt \qquad (24)$$

Feedback solution of this evaluation function J is as follows:

$$u = 8.3\Delta\omega - 0.0033\Delta\delta - 0.0030\Delta E_c - 0.0027\Delta E_{fd} - 0.34\Delta T_e \qquad (25)$$

Ignoring low-gain signals $\Delta\delta$, ΔE_c, ΔE_{fd}, and assuming $\Delta T_e \approx \Delta P_e$, the following multivariable feedback signal is obtained:

$$u = 8.3\Delta\omega - 0.34\Delta P_e \qquad (26)$$

Since the excitation system is thyristor based as shown in Fig. 2, when a system fault occurs, the thyristor output voltage reaches ceiling. Within the effective dynamic area of multivariable control PSS as represented in Eq. (26), however, the thyristor output voltage is linear. Hence, the evaluation function of Eq. (24) may be used without any problems. If ζ, set under q_ω = 500, happens to drop below 0.3 due to system impedance or specific characteristics of the generator and AVR, it will suffice to adjust the weight coefficient q_ω properly.

4. Computer Analysis

4.1 Confirmation of damping torque improvement

To estimate how much the multivariable control PSS improves damping torque, damping torque coefficient was calculated along a frequency band using Eqs. (25) and (26). The results are presented in Fig. 5. For the sake of comparison, also presented are characteristics in case of no PSS (AVR only) and conventional ΔP-PSS, the latter being described by:

$$W(S) = \frac{0.4(5S)^2 (1+0.1S)\ (1+2S)}{(1+5S)^2 (1+0.03S)\ (1+0.05S)\ (1+3.5S)} \qquad (27)$$

As is obvious from the diagram, the damping torque coefficient is over 30 at the natural frequency ω_n, for both ΔP-PSS and multivariable control PSS using Eqs. (25) and (26). Thus, the evaluation function of Eq. (24) proves to satisfy the condition of Eq. (20).

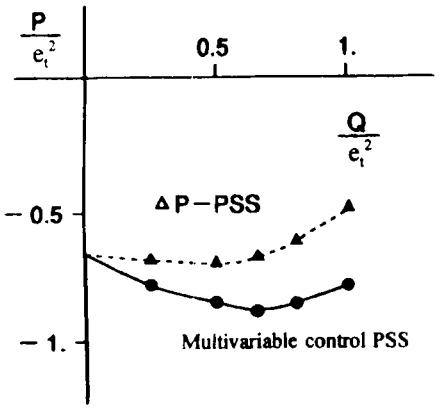

Fig. 6. Results of dynamic stability calculations at external impedance of 0.4 p.u.

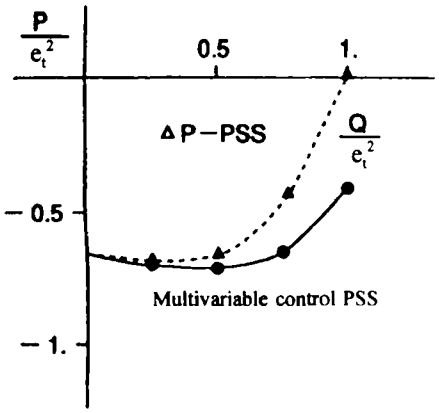

Fig. 7. Results of dynamic stability calculations at external impedance of 0.75 p.u.

As to the case of using AVR only, a very small positive value of the damping torque coefficient is indicative of extremely low stability.

4.2 Dynamic stability

Dynamic stability [11] refers to a certain area within which a stable operation is supported of the generator connected to the power system. In case of multivariable control PSS, if a stable operation area exists beyond a generator's performance curve such as

$$\left(\text{at } \frac{P}{e_t^2}=0.9 \quad \frac{Q}{e_t^2} \geqq 0.43 \ , \ \frac{Q}{e_t^2} \leqq -0.43\right)$$

stable operation of the generator is supported at any operating point. It was confirmed that multivariable control PSS, calculated using the evaluation function J of Eq. (24), offers the target value of damping torque coefficient. Besides, dynamic stability was examined using external impedance Xe as a parameter. In doing so, constants of generator and AVR were taken as shown in Table 1, and comparative calculations were made for multivariable control PSS described by Eq. (25), and ΔP-PSS described by Eq. (27). The results of dynamic stability calculations are presented in Figs. 6 and 7 for external impedance Xe of 0.4 p.u. and 0.75 p.u., respectively, while the external impedance is normally under 0.75 p.u. in most power systems.

In both cases with different external impedance, the multivariable control PSS offers a wider dynamic stability area compared to ΔP-PSS, and stability is assured during normal generator operation. The multivariable control PSS calculated after Eq. (26), with low-gain signals ignored in solution of Riccati equation, offers a dynamic stability area that is wider than the normal operating area for generators. This suggests that no problems of robustness are created by using Eq. (26) as an approximation of Eq. (25).

4.3 Transient stability

Simulations were carried out to estimate the damping effect of the multivariable control PSS in terms of transient stability, for both one-machine-to-infinite-bus system (used in design of the multivariable control PSS), and more realistic 4-machine system.

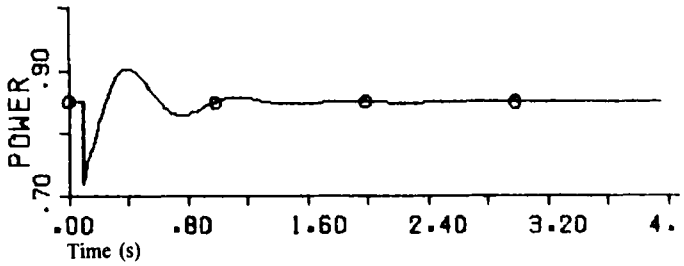

Fig. 8. Release of one circuit in one-machine-to-infinite-bus system with multivariable control PSS.

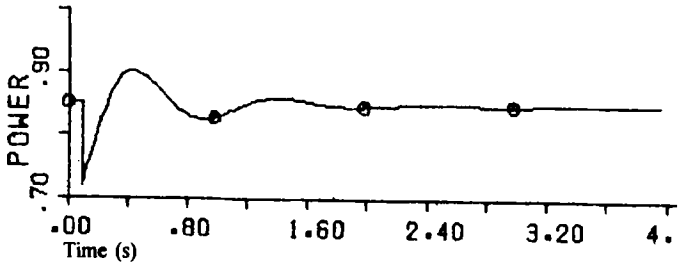

Fig. 9. Release of one circuit in one-machine-to-infinite-bus system with conventional ΔP-PSS.

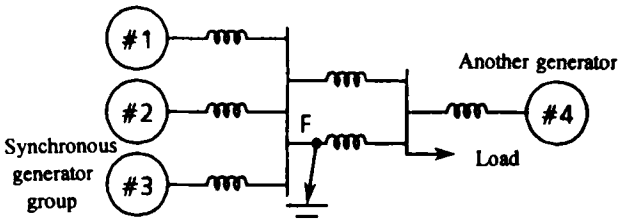

Fig. 10. Multigenerator configuration.

4.3.1 One-machine-to-infinite-bus system

Using simulation, multivariable control PSS was compared to ΔP-PSS in terms of power oscillation damping effect. Given in Figs. 8 and 9 are simulation results with one of the two transmission circuits in Fig. 1 released (as a disturbance), and system impedance Xe increased from 0.3 p.u. up to 0.4 p.u. As may be seen from the simulation with multivariable control PSS shown in Fig. 8, a good efficiency of power oscillation damping is offered; this corresponds to the damping torque shown in Fig. 5.

In the case of ΔP-PSS shown in Fig. 9, power oscillation, produced by disturbance, is damped quite well, but the damping effect is slightly lower than that of multivariable control PSS.

4.3.2 Multigenerator system

Shown in Fig. 10 is a configuration that includes three generators with multivariable control PSS connected with another generator. This configuration was employed to estimate power oscillation damping effect in the context of, first, step response in setting reference voltage for field tests on actual generator, and, second, study of transient stability by means of three-phase ground fault (3LG, point F in the diagram).

In the diagram, generators #1 ~ #3 are identical in rating, and employ the same excitation control system with multivariable control PSS. To estimate the effectiveness of multivariable control PSS in actual experiments, two cases were examined—with all three generators using only AVR, and with all three generators using multivariable control PSS. In either case, generators' voltage reference (denoted et_{ref} in Fig. 2) was changed stepwise, thus inducing power oscillation, and the attenuation coefficient was checked against Eq. (20). The results are presented in Figs. 11 and 12.

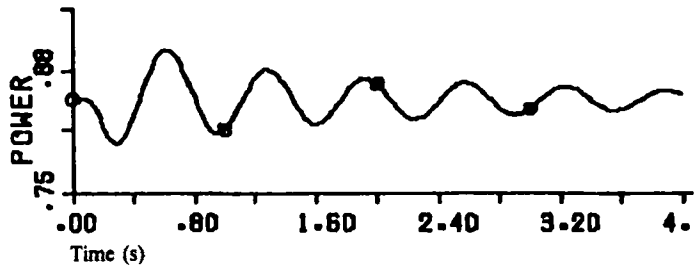

Fig. 11. Stepping-down of AVR reference for generator #3—only AVR.

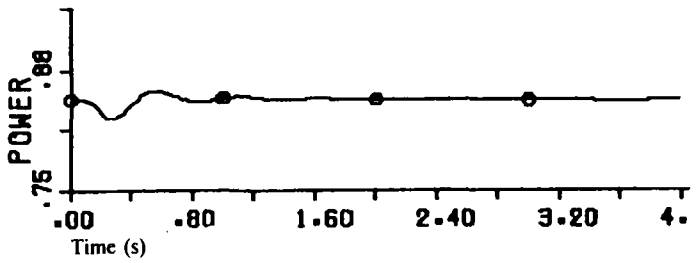

Fig. 12. Stepping-down of AVR reference for generator #3—using multivariable control PSS.

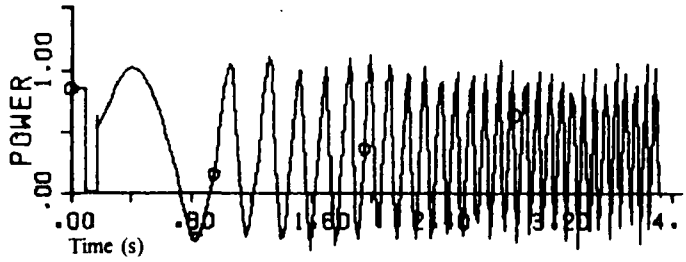

Fig. 13. Three-phase ground fault when using only AVR.

The AVR reference was stepped down for generator #3 only. As is evident from Fig. 11, with the generators controlled only by AVR, power oscillation attenuates and no instability occurs in operation. The simulation results for multivariable control PSS shown in Fig. 12 suggest a good damping effect for power oscillation. It was also confirmed that multivariable control PSS proved efficient in terms of transient stability, for instance, with three-phase ground fault. For this end, simulation was carried out for ground fault at point F in Fig. 10. The simulation of three-phase ground fault is shown in Fig. 13, with all three generators controlled with AVR only. As is evident from the diagram, stepout takes place. On the other hand, as shown in Fig. 14, simulation for generators using multivariable control PSS offers damping of power oscillation within two wavelengths after the ground fault is cleared.

5. Actual Application

Field tests were conducted to estimate the effect of multivariable control PSS when applied to actual generators. Shown in Fig. 15 is the excitation system configuration of actual generator, while the constants of generator and AVR were as in Table 1, and the test configuration was as shown in Fig. 10.

The AVR reference was stepped down, thus inducing power oscillation, and attenuation time of this power oscillation was used to estimate effectiveness of the multivariable control PSS. Shown in Figs. 16 and 17 are waveform records, respectively, when using AVR only, and when using multivariable control PSS.

The field test results shown in Figs. 16 and 17 check well with corresponding simulation results shown in Figs. 11 and 12, which proves that multivariable control PSS ensures efficient damping of power oscillation, in accord with design specifications. Although field tests have not been conducted for a variety of disturbances, from minor load changes to serious ground faults, a good damping effect may be expected for those disturbances as well.

6. Conclusions

In studies reported to date, the Riccati equation was applied to excitation control in order to improve stability, but in doing so, impracticable feedback signals were

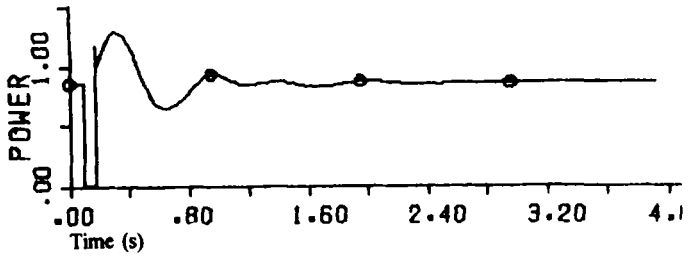

Fig. 14. Three-phase ground fault when using multivariable control PSS.

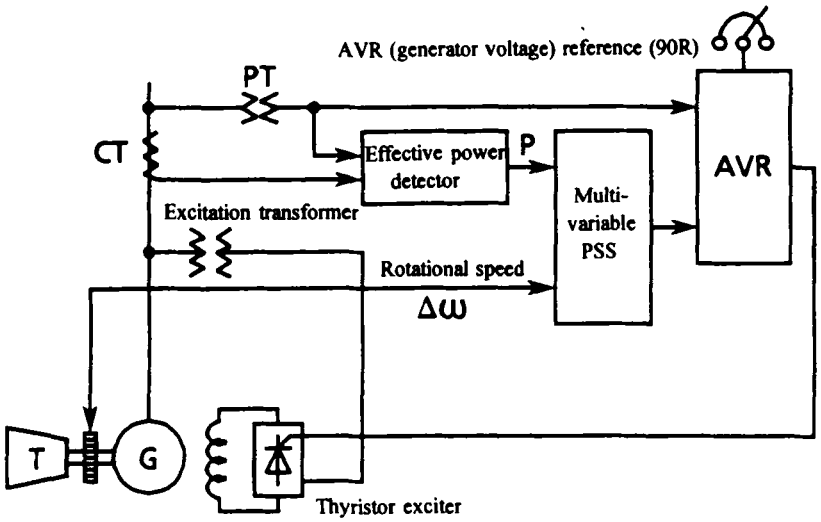

Fig. 15. Excitation system configuration of actual generator.

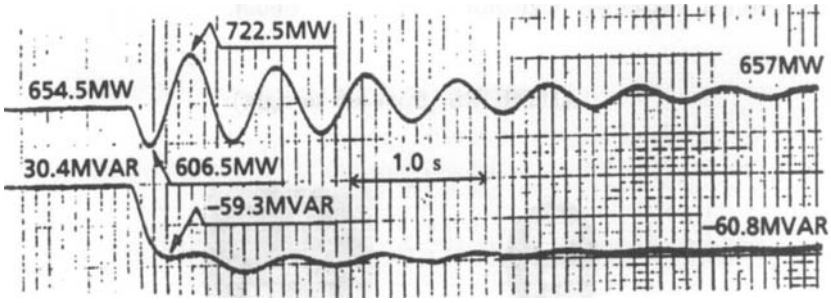

Fig. 16. Stepping-down of AVR reference for generator #3—AVR only.

employed, such as phase shift angle. In this paper, particular emphasis is made on $\Delta\omega$ that is related most closely to power oscillation, and the evaluation function is set according to the damping torque coefficient that is currently used to evaluate PSS, which allows for the design of a PSS signal set applicable to actual systems. Calculations of dynamic stability and transient stability prove that this multivariable control PSS outperforms conventional PSS in efficiency of power oscillation damping. Besides, the multivariable PSS was applied to

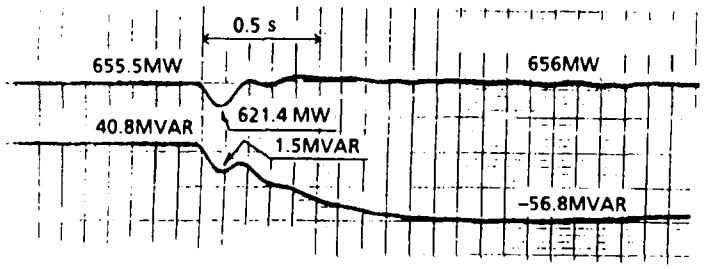

Fig. 17. Stepping-down of AVR reference for generator #3—using multivariable control PSS.

large-capacity 800 MVA tandem turbogenerator, and the field tests produced good results. At present, excitation systems using this multivariable control PSS are operating correctly.

REFERENCES

1. Kobayashi et al. Design technique and test results for a simple power system stabilizer. Trans. I.E.E., Japan, Vol. 33-B, p. 271, 1981.
2. L. Wedman and Y. Yu. Computation techniques for the stabilization and optimization of high order power system. IEEE PICA, p. 324, 1969.
3. Y. Yu. Application of an optimal control theory to a power system. IEEE Trans., Vol. PAS-89, p. 55, Jan. 1970.
4. Y. Yu and C. Sigger. Stabilization and optimal control signals for a power system. IEEE Trans., p. 1469, July 1970.
5. J. Bartlett. Performance of a 5-kVA synchronous generator with an optimal excitation regulator. PROC. IEE, Vol. 120, No. 10, p. 1250, Oct. 1973.
6. Saeki et al. Design of excitation systems based on quasi-optimal control theory. Trans. I.E.E., Japan, 5-B, p. 31, 1985.
7. A. Feliachi, X. Zhang and C. Sims. Power system stabilizers design using optimal reduced order models, Part 1. IEEE Trans., Vol. 4, No. 4, p. 1670, Nov. 1988.
8. A. Feliachi, X. Zhang and C. Sims. Power system stabilizers design using optimal reduced order models, Part 2. IEEE Trans., Vol. 4, No. 4, p. 1675, Nov. 1988.
9. Ohtsuka et al. Multivariable optimal control in generators. Trans. I.E.E., Japan, Vol. 86-B, p. 31, 1984.
10. F. Demello and C. Concordia. Concepts of synchronous machine stability as affected by excitation control. IEEE Trans., Vol. PAS-88, p. 316, April 1969.
11. Sekine. Theory of Power System Analysis. Denki Shoin.

AUTHORS (from left to right)

Kaiichiro Hirayama graduated in 1970 from Hokkaido University, Electrical Eng. Dept., and was employed by Toshiba Corp. He is engaged in development and design of power generating control systems. In 1994, he won Prize of Society of Instrument and Control Engineering. He received his Doctor of Engineering degree from Hokkaido University in 1995.

Yuichi Uemura graduated in 1977 from Hokkaido University, Electrical Eng. Dept., and was employed by Toshiba Corp. He is engaged in power system analysis.